



UNIVERSITY OF LEEDS

This is a repository copy of *Suppression of Auger Recombination in Nanocrystals via Ligand-Assisted Wave Function Engineering in Reciprocal Space.*

White Rose Research Online URL for this paper:  
<http://eprints.whiterose.ac.uk/129852/>

Version: Accepted Version

---

**Article:**

Califano, M [orcid.org/0000-0003-3199-3896](https://orcid.org/0000-0003-3199-3896) (2018) Suppression of Auger Recombination in Nanocrystals via Ligand-Assisted Wave Function Engineering in Reciprocal Space. The Journal of Physical Chemistry Letters, 9 (8). pp. 2098-2104. ISSN 1948-7185

<https://doi.org/10.1021/acs.jpcllett.8b00248>

---

© 2018 American Chemical Society. This document is the Accepted Manuscript version of a Published Work that appeared in final form in Journal of Physical Chemistry Letters, copyright © American Chemical Society after peer review and technical editing by the publisher. To access the final edited and published work see [insert ACS Articles on Request author-directed link to Published Work, see <https://doi.org/10.1021/acs.jpcllett.8b00248>].

**Reuse**

Items deposited in White Rose Research Online are protected by copyright, with all rights reserved unless indicated otherwise. They may be downloaded and/or printed for private study, or other acts as permitted by national copyright laws. The publisher or other rights holders may allow further reproduction and re-use of the full text version. This is indicated by the licence information on the White Rose Research Online record for the item.

**Takedown**

If you consider content in White Rose Research Online to be in breach of UK law, please notify us by emailing [eprints@whiterose.ac.uk](mailto:eprints@whiterose.ac.uk) including the URL of the record and the reason for the withdrawal request.



[eprints@whiterose.ac.uk](mailto:eprints@whiterose.ac.uk)  
<https://eprints.whiterose.ac.uk/>

# **Suppression of Auger recombination in nanocrystals via ligand-assisted wave function engineering in reciprocal space**

Marco Califano\*

*Pollard Institute, School of Electronic and Electrical Engineering, University of Leeds, Leeds LS2  
9JT, United Kingdom*

E-mail: [m.califano@leeds.ac.uk](mailto:m.califano@leeds.ac.uk)

---

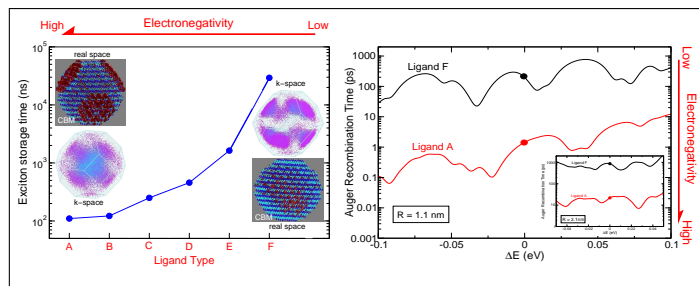
\*To whom correspondence should be addressed

## Abstract

A limiting factor to the technological application of conventional semiconductor nanostructures is their fast Auger recombination time. Strategies to increase it have so far mostly focused on decreasing the electron-hole wave function overlap *in real space* through structural modifications involving either elongation or shell growth.

Here we propose an alternative mechanism for Auger recombination suppression: a decrease in the overlap of electron and hole wave functions *in reciprocal space*.

# Graphical TOC Entry



Zero dimensional semiconductor nanocrystal quantum dots (NQDs) are nearly-spherical nanostructures which, owing to their 3D confinement, exhibit peculiar properties that set them apart from those of the bulk material from which they are made. However, while the size tunability of their optical properties and their inexpensive and relatively simple colloidal synthesis make them ideally suited for a wide range of device applications in very diverse fields,<sup>1-3</sup> the exploitation of their full potential in such applications is limited by the presence of a non-radiative multi-exciton decay mechanism which has proven especially efficient in these 0D systems, compared to the bulk and other low dimensional systems: Auger recombination (AR). Indeed, in commonly synthesized colloidal quantum dots, typical Auger recombination times range from a few to a few hundreds of picoseconds,<sup>4</sup> depending on the size. Such an efficient decay mechanism leads to large non-radiative losses, limits optical-gain lifetimes and spectral bandwidths for optical amplification, and is therefore detrimental for applications ranging from biolabelling to photovoltaics and lasing. Attempts to slow down Auger recombination have focused so far on the reduction of the overlap between electron and hole wave functions in real space,<sup>5</sup> achieved by structural modifications such as elongation (quantum rods,<sup>6</sup> quantum-dot-in-a-rod<sup>5</sup>) or shell growth (where a type II band alignment is formed at the heterointerface<sup>7,8</sup>). Core/giant-shell nanocrystals with a graded alloyed interface have also recently been shown to greatly inhibit Auger recombination,<sup>9</sup> an effect attributed to a “smoothing” of the confining potential at the heterointerface.<sup>10</sup> This procedure allows reductions in the Auger recombination rates of two orders of magnitude or more, at the expense, however, of a complex synthetic method (successive ion layer absorption and reaction - SILAR) requiring long growth periods.<sup>9</sup>

The question we will address here is whether Auger recombination can be efficiently suppressed without resorting to such time-consuming and costly procedures and, above all, without modifying the morphology of the nanocrystal.

A promising strategy to achieve this goal is the modification of the nanocrystal surface

*chemistry*. Indeed, as a consequence of their chemical nature, NQDs are surrounded by a very complex environment, their surface being in contact with various chemical species present in solution and different organic capping molecules, whose presence is needed to ensure solubility, prevent aggregation and passivate surface dangling bonds.<sup>11,12</sup> Specific capping groups are, however, also known to introduce localized states on the surface, which can act as traps for either electrons or holes.<sup>13</sup> Furthermore, the concentration<sup>14</sup> and the quantity<sup>15</sup> of surface ligands has been shown to be important, where deviations from an optimal number lead to the formation of defect states in the gap.<sup>15</sup>

It was also recently shown experimentally<sup>16</sup> that different capping agents could shift the ionization energy of an ensemble of 4.7 nm diameter CdSe NQDs by up to 0.35 eV, equivalent to the shift caused by a size (i.e. diameter) reduction of nearly 3 nm; other groups<sup>17</sup> have shown similar shifts (up to 0.3 eV) in the ionization potential and the local vacuum level in tethered 3.6 and 6.0 nm diameter CdSe dots, depending on the capping group. Similarly, in InAs nanocrystals with 4.4 nm diameter, exchange of native trioctylphosphine (TOP) ligands with 4-methylthiophenol (MTP) and aniline, led to shifts of the highest occupied molecular orbital (HOMO) by 0.2-0.3 eV and 0.3-0.4 eV respectively.<sup>18</sup> Other studies have found that surface ligands can affect the optical properties in CdSe nanocrystals<sup>19,20</sup> (where the same ligand can have opposite effects, i.e., enhance the PL or quench it, depending on the surface stoichiometry of the nanocrystal<sup>21</sup>), the rate of electron intra-band relaxation in CdSe solutions,<sup>22</sup> the intensity of surface emission in CdSe dots,<sup>23</sup> the optical band gap and the exciton confinement in CdS, CdSe, PbS<sup>24</sup> and CdTe nanocrystals,<sup>25</sup> and even modify the stoichiometry<sup>26</sup> or the overall morphology<sup>27</sup> of lead chalcogenide nanocrystals. The specific surface chemistry of the NQD has also been recently found responsible for other more subtle, but by no means less important, effects, such as the control of the band-edge exciton linewidth.<sup>28</sup> All these effects impact the nanocrystal's structure and/or its energetics. So far, however, apart from the creation or removal from the gap of surface trap states, no indication was found experimentally

that the ligand's presence could interfere with the core electron and hole wave functions to such an extent as to result in a sufficient reduction in their overlap to suppress any recombination mechanism to any degree.

An indication that this could be possible was provided by Reboredo and Zunger,<sup>29</sup> who found theoretically that the exciton radiative lifetime in Ge NQDs could be modified by changing the electronegativity of the nanocrystal's passivating potentials. Although in that case the main origin of the predicted long exciton lifetimes was a change in the orbital symmetry of the VBM (which modified the allowed/forbidden character of the lowest excitonic manifold), they also predicted a change in the Bloch-function composition in reciprocal space, from X to L, of the CBM wave function. Similarly, Poddubny and Dohnalová<sup>30</sup> recently suggested the possibility of promoting direct-like band gap transitions in Si NQDs (achieving over-2-orders-of-magnitude enhancements in the radiative rates), by modifying their surface electronegativity.

These results hint to the tantalizing possibility of manipulating the wave functions in reciprocal space through a simple ligand exchange procedure.

For such a manipulation to be effective, favourable conditions are: (i) a bulk band structure featuring energetically closely spaced minima in the conduction band; (ii) large differences between their effective masses; (iii) large values for the exciton Bohr radius. There are a few materials that match these criteria (GaSb, GaAs, InP, and InSb). We chose GaSb, which, although not presently synthesised colloiddally, exhibits many peculiar properties in the bulk that make it a promising candidate for device application at the nanoscale. In particular, the separation between the conduction band minimum (CBM) at  $\Gamma$  and the slightly higher minima at the L-points is only about 80 meV, whereas the ratio of the effective masses at these high symmetry points is larger than 2.<sup>31</sup> It is therefore expected that confinement should induce a  $\Gamma$ -to-L transition in the character of the conduction band minimum, similarly to what was predicted to occur in GaAs,<sup>32</sup> where, however, the  $\Gamma$ -L and  $\Gamma$ -X separations are much larger (300 eV and 460 eV, respectively)

and the exciton Bohr radius is nearly half of that in GaSb. The valence band of GaSb, instead, has the structure common to all zinc-blende semiconductors, hence its  $\Gamma$  character is not expected to change with confinement. As a consequence, a confinement-induced reduction of band edge electron and hole wave function overlap *in reciprocal space* is expected in this material, which could lead to a suppression of Auger recombination rates in GaSb NQDs of suitable sizes. At the same time confinement should also induce a direct-to-indirect band gap transition in these nanostructures which should result in long exciton storage times.

The important question to ask, however, is whether the CBM composition (hence the electron and hole wave function overlap) *in reciprocal space* can be modified via ligand exchange for the *same nanocrystal size*.

We consider nanocrystals with two different sizes,  $R = 1.1$  nm and  $R = 2.1$  nm, which are built with bulk-like crystal structure, starting from a central anion, up to the desired radius  $R$ . This procedure yields unsaturated bonds at the dot surface, which are passivated here by 6 different sets (indicated by the capital letters A to F) of pseudo-hydrogenic, short-range potentials with Gaussian form,

$$v(\mathbf{r}) = \alpha e^{-(|\mathbf{r}-\mathbf{R}(\gamma)|/\sigma)^2} \quad (1)$$

chosen to reproduce specific effects (see below) of realistic capping groups. Each model ligand is characterized by (i) the amplitude  $\alpha$  and (ii) the width  $\sigma$  of the Gaussian potential, and by (iii) the distance  $\gamma d$  from the surface atom along the ideal bond line connecting it with the missing atom ( $d$  is the bond length and  $\mathbf{R}(\gamma)$  is the ligand position).<sup>33–35</sup> This is clearly an oversimplified model for a complex organic molecule. Nevertheless, it is sufficiently detailed to capture the essential properties of the capping agent’s most important component: its binding moiety. Indeed, as it will be discussed later on in the paper, it has been shown experimentally<sup>16,18</sup> that it is this part of the ligand that exhibits the properties

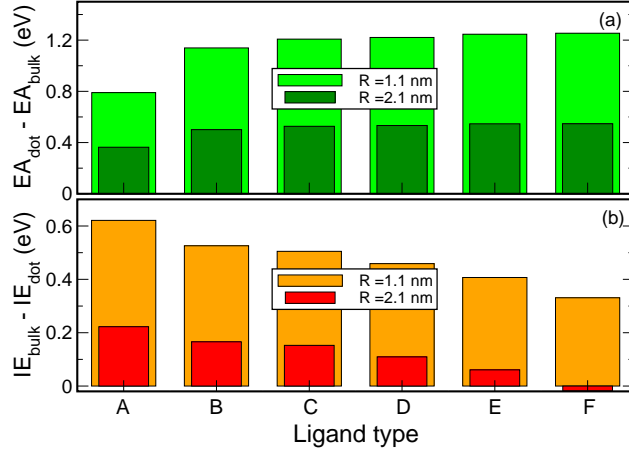


Figure 1: Electron affinity and ionization energy dependence on surface ligand for GaSb NQDs with  $R = 1.1$  nm and  $R = 2.1$  nm (both quantities are reported relative to the bulk values).

responsible for the features we are interested in.

Both anion and cation surface atoms are passivated using the same procedure in order to remove the corresponding trap states from the gap. However, we only vary the cation passivation parameters  $\alpha$  and  $\gamma$  in sets A to F (see Supporting Information), to model different realistic ligands, as the capping groups usually bind to the metal atom on the surface<sup>36</sup> (Further details on the method can be found in the Supporting Information).

### Nanocrystal's ionization energy and electronegativity of the binding moiety

The effects of these 6 ligand typologies on the electron affinities (defined as  $EA = E_{\text{vacuum}} - E_{\text{cbm}}$  - green bars), and ionization energies (defined as  $IE = E_{\text{vacuum}} - E_{\text{vbm}}$  - red and orange bars) of both GaSb nanocrystal sizes is shown in Figure 1. The range of ligand-induced variations in the IEs calculated here (290 meV and 241 meV for  $R = 1.1$  nm and  $R = 2.1$  nm, respectively) is comparable to that observed in CdSe (300 meV<sup>17</sup> to 350 meV<sup>16</sup>), and InAs (400 meV),<sup>18</sup> suggesting that our model ligands reproduce realistically the behaviour of a variety of real capping groups.

From Figure 1 it is also clear that ligands A to F have an increasingly confining effect on the electron, consistently with the parameters that characterise them (see Table S1, Supporting Information), as they progressively shift the conduction band edge towards

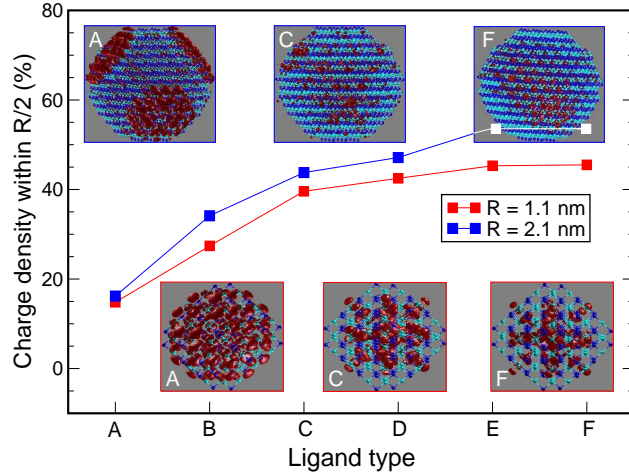


Figure 2: Main panel: Fraction of electron CBM charge density contained within a sphere of radius  $R/2$  from the dot centre for NQDs with  $R = 1.1$  nm (red squares and line) and  $R = 2.1$  nm (blue squares and line). Top insets: 3D electron charge density in a  $R = 2.1$  nm radius GaSb nanocrystal capped by ligands A, C and F. Bottom insets: 3D electron charge density in a  $R = 1.1$  nm radius GaSb nanocrystal capped by ligands A, C and F. The blue and cyan spheres represent Ga and Sb atoms, respectively.

higher levels (i.e., away from the bulk band edge), while, at the same time, decreasing the valence band edge distance from the bulk value. These results therefore highlight the close link between electron confinement and IE. Such an increased confining effect, obtained without reducing the nanocrystal size, is precisely the feature required to achieve the desired increase in the  $L$  content of the electron wave function.

The extent of the ligands' influence on the carrier's localisation is further characterised in Figure 2, where we plot the fraction of the CBM electron charge density contained within a sphere of radius  $R/2$  from the dot centre. As the volume of such a sphere is  $1/8$  of the total dot volume, if the carriers were distributed uniformly throughout the nanostructure, we would expect to find 12.5% of their density there. This seems to be the case for a ligand-A capping in both dots, whereas the relative charge density increases steadily for dots passivated with B to F (up to about 45% in the smaller dot, and to 54% in the larger dot), consistently with the increased electron confinement deduced from the calculated electron affinities (Figure 1). An inspection of the 3D CBM charge densities (shown for selected passivants - A, C and F - in the top and bottom panels of Figure 2),

and of the CBM density profiles calculated for passivants A and F (Figure S1, Supporting Information), however, reveals that, far from being uniformly distributed, the electron charge density relative to dots capped by ligand A exhibits a larger concentration close to the surface, on atomic planes rich in Ga atoms with two dangling bonds. The opposite is true for nanocrystals whose surface is terminated by passivant F, where the largest concentration occurs at the dot centre. We therefore conclude that ligands from F to A display an increasing efficiency to attract the electron, i.e., increasing electronegativity. This causal link between the ligand's electronegativity and the resulting shift in the nanocrystal's IE is consistent with the available experimental evidence.<sup>16,18</sup> Indeed, Soreni-Harari *et al.*<sup>18</sup> linked the shifts they observed in the HOMO energy of InAs NQDs terminated by different ligands with the electronegativity of their binding moiety (with the more electronegative anchor group inducing the largest IE). They concluded that the most important role in determining the shift was played by the binding moiety itself, by failing to observe any correlation between the capping molecule's polar terminal group and the shift induced. A similar conclusion was reached by Jasieniak *et al.*,<sup>16</sup> regarding the ionization energy in CdSe NQDs capped with different ligands, where variations in surface moiety were found to induce changes from 0.05 eV up to 0.35 eV, whereas no appreciable changes were induced by variations of the alkyl chain length for each of the moieties. This evidence also directly confirms the suitability of our simplified ligand model for the purposes here investigated. Based on these results and on the analysis proposed for InAs NQDs,<sup>18</sup> given the similarity in magnitude of the shifts we calculate to the experimentally observed ones, we therefore expect: (i) our A-F ligands to model *real* ligands featuring different binding groups; (ii) the ligand producing the largest shift (A, see Figure 1) to replicate the characteristics of the passivant with the most electronegative anchor group in the set; and (iii) ligands producing increasingly smaller shifts to model real ones having moieties with decreasing values of electronegativity.

It would be interesting now to identify ligands A-F with real ligands. Unfortunately,

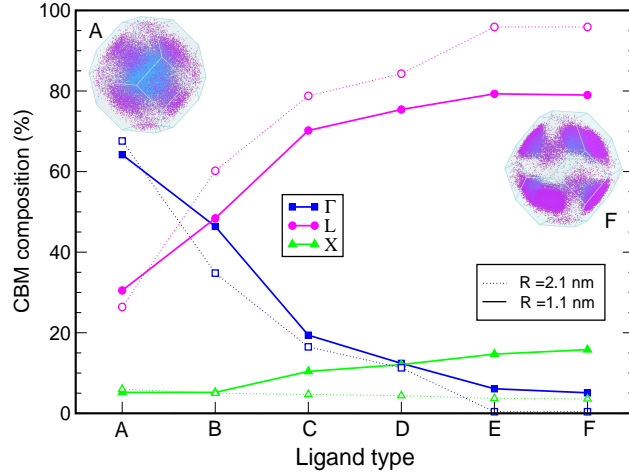


Figure 3: k-vector decomposition of the CBM wave functions for  $R = 1.1$  nm (solid lines and full symbols) and  $R = 2.1$  nm (dotted lines and empty symbols) NQDs:  $\Gamma$ , blue squares; L, magenta circles; and X, green triangles (the lines are a guide to the eye). The insets display the 3D Brillouin zone calculated for a  $R = 2.1$  nm NQD capped by ligands A and F, where the k points are color coded according to the main panel: blue, close to  $\Gamma$  and magenta, close to L.

as we repeatedly stressed, our approach only allows us to model the properties of the ligand's binding group. Therefore, proceeding further to assign a specific molecule to each of our model ligands would involve a large degree of uncertainty and arbitrariness. This task is complicated even further by the lack of consensus in the literature on the viable passivations for Ga-based nanocrystals: while Alivisatos' and Weller's groups used trioctylphosphine (TOP)<sup>52</sup> and trioctylphosphine oxide (TOPO)<sup>53</sup> as surfactants for their GaAs and GaP nanocrystals, recent attempts by Talapin's group to stabilize GaAs nanocrystals with traditional organic ligands (including, apart from TOP and TOPO, also various combinations of oleylamine or hexadecylamine, oleic acid, dodecanethiol, and octadecylphosphonic acids) proved unsuccessful.<sup>54</sup> Therefore, having shown that our model ligands are realistic, we are however unable to identify them with specific capping molecules.

### **Analysis of the electron wave function in reciprocal and real space**

As discussed above, in GaSb the extent of the ligands' influence on the k-space composi-

tion of the nanocrystal's core states is expected to be linked to the IE shifts they induce, since to small values of the IE correspond increased confinement and *vice versa*, and confinement is expected to affect the character of the CBM in reciprocal space. The results of a k-vector decomposition of the conduction band edge wave function in terms of high-symmetry point components, presented in Figure 3, show a strong ligand dependence of the  $\Gamma$  and L contributions to the CB wave functions. The confinement-induced  $\Gamma$ -to-L transition of the GaSb CBM, expected to take place in much larger dots,<sup>37</sup> is strongly inhibited by ligand A and only slightly allowed by ligand B (for which  $\Gamma$  and L contributions have almost equal magnitude), in the smaller dot. Nanocrystals capped with ligands C-F show instead CBMs with majority L character, which increases from C to F (as does their confining effect), and, accordingly, decreasing contributions from  $\Gamma$ . A very similar behavior is exhibited by the larger dot, where it is also accompanied by a change in the CBM envelope function symmetry, from prevalently *s*-like, for dots capped with ligands A - D, to *p*-like, for dots terminated by ligands E and F. The VBM envelope is found instead to be *s*-like only for ligand A, whereas its symmetry is *p*-like for all other ligands (further details on the symmetry of the band edges can be found in the Supporting Information).

### **Exciton and multi-exciton recombination rates**

The  $\Gamma$ -to-L transition in the CBM character should lead to a reduction in the CBM-VBM wave function overlap (and to a direct-to-indirect band gap transition) in reciprocal space, since the VBM remains mainly  $\Gamma$ , irrespective of surface termination. As a consequence, the Auger recombination time and the exciton radiative lifetime are expected to increase from dots capped with ligand A (exhibiting a  $\Gamma$ -like CBM), to F, where the L character is most pronounced.

Our results, presented in Figure 4, Figure 5 (black squares and line) and Figure S2 (Supporting Information), confirm these expectations, showing an astonishing over-two-orders-of-magnitude suppression of Auger recombination (i.e., comparable to that achieved, using much more complex synthetic procedures, in core/giant-shell nanostructures<sup>38</sup>),

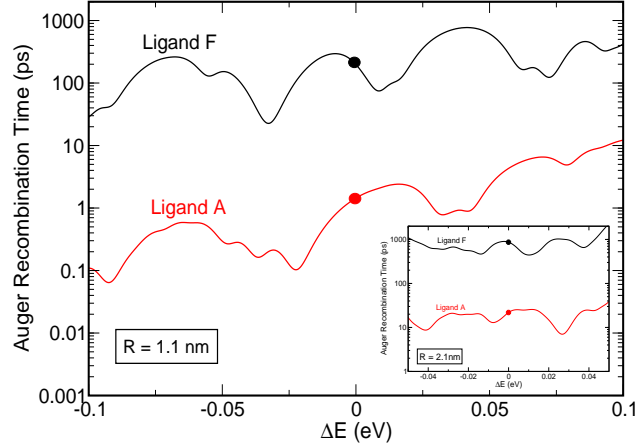


Figure 4: Auger recombination times in toluene calculated for GaSb NCDs with  $R = 1.1$  nm, capped with ligands A (red line) and F (black line), as a function of the variation in the band gap energy around the value ( $\Delta E = 0$ ) predicted for that specific size.  $\Delta E$  accounts for ensemble structural effects (size distribution or shape anisotropy) and the influence of the nanocrystal environment (local electric fields and/or charge fluctuations). The inset displays the results for  $R = 2.1$  nm. For illustrative purposes, the range of variation for  $\Delta E$  shown (100 meV and 50 meV for  $R = 1.1$  nm and  $R = 2.1$  nm, respectively) is larger than realistically expected.

and a nearly-three-orders-of-magnitude increase in lifetime from A- to F-capped dots for both sizes considered. In Figure 4, where the AR time is shown as a function of the variation  $\Delta E$  in the band gap energy around the value ( $\Delta E = 0$ ) predicted for the specific sizes considered,<sup>39</sup> the AR time calculated at  $\Delta E = 0$  for a  $R = 1.1$  nm dot ranges from 1.5 ps, for capping with ligand A, to about 200 ps, for ligand F termination. Its largest variation (occurring within less than one LO phonon energy from  $\Delta E = 0$ ) spans however 3 orders of magnitude, from 0.1 ps to 100 ps, whereas the longest calculated AR time approaches the ns range in F-terminated NQDs. Similarly, in a dot with  $R = 2.1$  nm, the AR time at  $\Delta E = 0$  ranges from 22 ps (ligand A) to 866 ps (ligand F); whereas the largest variation (still within  $\hbar\omega_{LO}$  from  $\Delta E = 0$ ) is from 7 ps to 1013 ps, reaching into the ns range for F-capped nanocrystals. In comparison, InAs and InSb NQDs with  $R = 2.1$  nm exhibit AR times of a few ps.<sup>40–43</sup>

From simple bulk scaling arguments<sup>4</sup> it can be shown that the tri- and quadri-exciton recombination times  $\tau_3$  and  $\tau_4$  satisfy  $\tau_4 : \tau_3 : \tau_2 = 0.25 : 0.44 : 1$  and can therefore be pre-

dicted from the calculated bi-exciton AR times  $\tau_2$ . Our results show that 4-exciton AR times in GaSb nanocrystals with  $R = 2.1$  nm can be engineered to exceed 200 ps, by using appropriate capping agents. In contrast,  $\tau_4$  values measured in CdSe dots of similar sizes are of the order of a few ps, i.e., about two orders of magnitude faster.<sup>4</sup>

It should be noted that, since a specific passivant modifies both AR and PL times in the same direction (i.e., F increases both, A decreases both), F-terminated nanocrystals will be ideally suited for applications requiring long carrier lifetimes, such as PV or bio-labelling (a new time-gated immunofluorescence imaging method<sup>49</sup> was recently made possible by NQDs with photoluminescence lifetimes in the  $\mu$ s range). On the other hand, as in such nanocrystals the radiative lifetime increases more than AR lifetime, they will exhibit a lower biexciton quantum yield<sup>50</sup> (reduced by a factor of 2 in the smaller structures and nearly by one order of magnitude in GaSb nanocrystals with  $R = 2.1$  nm) than A-capped dots, which will be therefore better suited for applications such as LEDs, single photon sources and lasers. In this respect, it is however interesting to note that even core/giant-shell nanocrystals exhibiting complete blinking suppression<sup>9</sup> can exhibit<sup>51</sup> biexciton quantum yields  $\ll 0.1$ , and, hence, a much reduced degree of AR suppression.

### **Excitonic structure and Stokes shifts**

A further origin for the lifetimes increase we predict is the symmetry change of both VBM and CBM (whose implications on the optically allowed or forbidden character of the excitonic states derived from them are discussed in the Supporting Information). In nanocrystals capped by ligand A we find that the ground state exciton is dark. However, the bright exciton is only 0.15 meV higher in energy (i.e., thermally populated for  $T > 1.7$  K), leading to a short radiative lifetime. As a stronger transition with a larger oscillator strength is located higher in energy, we find a significant global Stokes shift (70 meV)<sup>44</sup> in this case. For surface terminations types B to D, the ground state exciton has instead a dipole-allowed component, yielding a partially allowed ground exciton, with a much longer lifetime than the fully allowed, bright exciton found in dots passivated by ligand

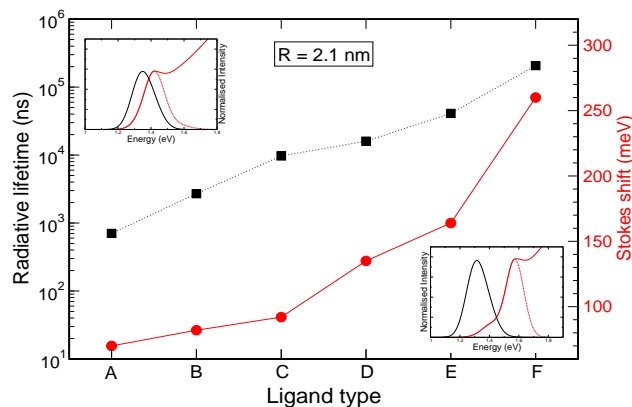


Figure 5: Room temperature radiative recombination times (black squares and line - left y axis), in toluene, and Stokes shifts (red circles and line - right y axis) calculated for NCDs with  $R = 2.1$  nm, capped with different ligands A-F (The lines are a guide to the eye). The insets display the calculated normalised emission (black line) and absorption (red line) spectra (assuming a Gaussian broadening of 80 meV) for ligand A (top left) and F (bottom right). The red solid lines show the calculated absorption superimposed on a background increasing as the third power of the energy, whereas the red dashed lines show the Gaussian curve alone.

A. The Stokes shift calculated for dots capped by these ligands follows the trend of the lifetimes, as a result of the progressive shift to higher energies of the fully allowed optical transitions. Finally, for large dots capped by ligands E and F, the symmetry of the band edges leads to a manifold of over 100 dark exciton states, (including degeneracies), starting from the ground state upwards, yielding (a) the longest lifetime calculated for this dot size, nearly 3 orders of magnitude larger than for A-capped dots, and (b) the larger Stokes shift, above 250 meV, for F-capped dots (see Figure 5 red circles).

Large separations between emission and band edge absorption (referred to as “global Stokes shifts”) suppress photoluminescence self-absorption and are therefore beneficial to all applications exploiting light emitted from the dot (LEDs, biological imaging,<sup>49</sup> lasers, solar energy harvesting,<sup>45,46</sup> etc.). Although the Stokes shifts obtained here are smaller than those achievable using core/giant-shell nanocrystals,<sup>45</sup> or dopants,<sup>47</sup> their tunability through the choice of the surface termination presents a simpler synthetic alternative.

### Comparison with available experimental data

To the best of our knowledge there are no available systematic experimental studies on the effect of different capping groups on AR rates. There are however studies on the effect of ligands on intraband electron relaxation, which in colloidal nanocrystals can be due (and is generally attributed<sup>48</sup>) to an Auger process. It is reasonable to assume that the reduced overlap in reciprocal space responsible for the AR suppression discussed here, will apply to Auger electron cooling (AC) as well, given that the evaluation of the rate of the latter involves the calculation of matrix elements containing both electron and hole band edge wave functions. Therefore our AR suppression strategy could be indirectly verified using electron intraband relaxation data. A progressive increase in the electron decay times measured in CdSe nanocrystals capped by tetradecylphosphonic acid (TDPA), TOPO, oleic acid (OA), oleylamine (OLA), and n-dodecanethiol (DDT), respectively, was indeed reported by Guyot-Sionnest *et al.*<sup>22</sup> Considering that the electronegativity of the binding moiety of these ligands decreases from TDPA to DDT, these observations are consistent with our model. Furthermore, they suggest (a) that the applicability of our strategy extends to most materials, irrespective of whether their bulk band structure exhibits closely-spaced minima in the conduction band (condition (i) above) or not, but also (b) that the extent of the Auger rates suppression does indeed depend on the band structure (in the case of CdSe, where there are no closely spaced minima, the observed increase in the decay times was found<sup>22</sup> to be at most a factor of 7, from 3.8 ps to 27 ps, for 4.5 nm NQDs, compared to the orders of magnitude increase we predict in GaSb). Similar considerations should also apply to the material's optical properties, as was recently reported for Si NQDs.<sup>55</sup>

It has to be mentioned that Guyot-Sionnest and co-workers interpreted their results in terms of "energy transfer to electronic states mediated by the interfacial polarity or energy transfer to high-frequency vibrations of the ligands."<sup>22</sup> We note, however, that, as in these experiments it was not possible to isolate the binding moiety (whose electronegativity may have influenced the AC rates) from the rest of the ligand molecule (which

was responsible for the high-frequency vibrations), and the surrounding environment, it is difficult to determine to what extent each of these factors contributed to the observed increase in the decay times. The picture is further complicated by the fact that surface interactions in real samples are still poorly understood, despite the large number of studies (both experimental and theoretical) on this subject. In our study we isolated the binding moiety from the rest of the molecule, supported by experimental evidence that (i) this is the main factor that determines the shift in ionization energy and (ii) this shift is linked to the moiety's electronegativity. We then proceeded to show that our model ligands could reproduce the magnitude of the shifts produced by different real ligands in different materials, hence they were realistic models for the binding moieties of such ligands. Finally we linked the moiety's electronegativity with the k-space character of the electron wave function and this to the AR rates.

In conclusion, we have presented a new, very simple and effective strategy to tune radiative and non-radiative decay rates within an orders-of-magnitude-wide range, by modifying the reciprocal space composition of the band edge states wave functions through surface chemistry manipulation. Indeed, we found that by varying the electronegativity of a ligand's binding moiety it is possible to reproduce the effects of confinement - where less electronegative anchor groups induce increased confinement and *vice versa* - hence to induce variations in the symmetry and the k-space character of a core state, in materials where the separation between two or more high-symmetry points in the bulk band structure is small. As a consequence, (i) Auger recombination can be suppressed to a degree comparable to that achieved in core/giant-shell nanocrystals; (ii) the radiative lifetime in the nanocrystal may be tailored to vary within nearly three orders of magnitude, while (iii) the Stokes shift can be engineered to suppress PL self-absorption, by simple ligand exchange procedures. This will enable a fuller exploitation of these nanostructures in a wide variety of fields from photovoltaics to biological imaging.

## Supporting Information Available

The parameters relative to the different model ligands A-F (Table SI); Method; Charge Density profiles calculated for a NQD with  $R = 2.1$  nm capped with ligands A and F (Figure S1); Symmetry of the band edge wave functions and character of the ground state excitonic transitions; Radiative lifetimes calculated for a NQD with  $R = 1.1$  nm capped with ligands A and F (Figure S2).

## References

- (1) Talapin, D. V.; Lee, J.-S.; Kovalenko, M. V.; Shevchenko, E. V. Prospects of Colloidal Nanocrystals for Electronic and Optoelectronic Applications *Chem. Rev.* **2010**, *110*, 389-458
- (2) Kovalenko, M. V. *et al.* Prospects of Nanoscience with Nanocrystals *ACS Nano* **2015**, *9*, 1012-1057.
- (3) Kagan, C. R.; Lifshitz, E.; Sargent, E. H.; Talapin, D. V. Building Devices from Colloidal Quantum Dots. *Science* **2016**, *353*, aac5523.
- (4) Klimov, V. I.; Mikhailovsky, A. A.; McBranch, D. W.; Leatherdale, C. A.; Bawendi, M. G. Quantization of Multiparticle Auger Rates in Semiconductor Quantum Dots. *Science* **2000**, *287*, 1011-1013.
- (5) Zavelani-Rossi, M.; Lupo, M. G.; Tassone, F.; Manna, L.; Lanzani, G. Suppression of biexciton Auger recombination in CdSe/CdS dot/rods: role of the electronic structure in the carrier dynamics. *Nano Lett.* **2010**, *10*, 3142-3150.
- (6) Htoon, H.; Hollingsworth, J. A.; Dickerson, R.; Klimov, V. I. Effect of zero- to one-dimensional transformation on multiparticle Auger recombination in semiconductor quantum rods *Phys. Rev. Lett.* **2003**, *91*, 227401.

- (7) Oron, D.; Kazes, M.; Banin, U. Multiexcitons in type-II colloidal semiconductor quantum dots. *Phys. Rev. B* **2007**, *75* 035330.
- (8) Osovsky, R.; Cheskis, D.; Kloper, V.; Sashchiuk, A.; Kroner, M.; Lifshitz, E. Continuous-Wave Pumping of Multiexciton Bands in the Photoluminescence Spectrum of a Single CdTe-CdSe Core-Shell Colloidal Quantum Dot. *Phys. Rev. Lett.* **2009**, *102*, 197401/1-197401/4.
- (9) Chen, Y.; Vela, J.; Htoon, H.; Casson, J. L.; Werder, D. J.; Bussian, D. A.; Klimov, V. I.; Hollingsworth, J. A. "Giant" Multishell CdSe Nanocrystal Quantum Dots with Suppressed Blinking. *J. Am. Chem. Soc.* **2008**, *130*, 5026-5027.
- (10) Cragg, G. E.; Efros, A. L. Suppression of Auger Processes in Confined Structures. *Nano Lett.* **2010**, *10*, 313-317.
- (11) Boles, M. A.; Ling, D.; Hyeon, T.; Talapin, D. V. The Surface Science of Nanocrystals *Nat. Mater.* **2016**, *15*, 141-153.
- (12) Green, M. The Nature of Quantum Dot Capping Ligands *J. Mater. Chem.* **2010**, *20*, 5797-5809.
- (13) Houtepen, A. J.; Hens, Z.; Owen, J. S.; Infante, I. On the Origin of Surface Traps in Colloidal II-VI Semiconductor Nanocrystals. *Chem. Mater.* **2017**, *29*, 752-761.
- (14) Munro, A. M.; Plante, I. J. L.; Ng, M. S.; and Ginger, D. S. Quantitative Study of the Effects of Surface Ligand Concentration on CdSe Nanocrystal Photoluminescence *J. Phys. Chem. C* **2007**, *111*, 6220-6227
- (15) Kim, D.; Kim, d.-H.; Lee, J.-H.; Grossman, J. C. Impact of Stoichiometry on the Electronic Structure of PbS Quantum Dots. *Phys. Rev. Lett.* **2013**, *110*, 196802.
- (16) Jasieniak, J.; Califano, M.; Watkins, S. E. Size-Dependent Valence and Conduction Band-Edge Energies of Semiconductor Nanocrystals *ACS Nano* **2011**, *5*, 5888-5902.

- (17) Munro, A. M.; Zacher, B.; Graham, A.; Armstrong, N. R. Photoemission Spectroscopy of Tethered CdSe Nanocrystals: Shifts in Ionization Potential and Local Vacuum Level As a Function of Nanocrystal Capping Ligand *ACS Appl. Mater. Interfaces* **2010**, *2*, 863-869.
- (18) Soreni-Harari, M.; Yaacobi-Gross, N.; Steiner, D.; Aharoni, A.; Banin, U.; Millo, O.; Tessler, N. Tuning Energetic Levels in Nanocrystal Quantum Dots through Surface Manipulations. *Nano Lett.* **2008**, *8*, 678-684.
- (19) Talapin, D. V.; Rogach, A. L.; Kornowski, A.; Haase, M.; and Weller, H. Highly Luminescent Monodisperse CdSe and CdSe/ZnS Nanocrystals Synthesized in a Hexadecylamine-Trioctylphosphine Oxide-Trioctylphosphine Mixture *Nano Lett.* **2001**, *1*, 207-211.
- (20) Kalyuzhny, G. and Murray, R. W. Ligand Effects on Optical Properties of CdSe Nanocrystals. *J. Phys. Chem. B* **2005**, *109*, 7012-7021.
- (21) Jasieniak, J.; Mulvaney, P. From Cd-Rich to Se-Rich - the Manipulation of CdSe Nanocrystal Surface Stoichiometry. *J. Am. Chem. Soc.* **2007**, *129*, 2841-2848.
- (22) Guyot-Sionnest, P.; Wehrenberg, B.; Yu, D. Intraband Relaxation in CdSe Nanocrystals and the Strong Influence of Surface Ligands. *J. Chem. Phys.* **2005**, *123*, 074709.
- (23) Krause, M. M.; Jethi, L.; Mack, T. G.; and Kambhampati, P. Ligand Surface Chemistry Dictates Light Emission from Nanocrystals. *J. Phys. Chem. Lett.*, **2015**, *6*, 4292-4296.
- (24) Frederick, M. T.; Amin, V. A.; Cass, L. C.; Weiss, E. A. A Molecule to Detect and Perturb the Confinement of Charge Carriers in Quantum Dots *Nano Lett.* **2011**, *11*, 5455-5460.
- (25) Akamatsu, K.; Tsuruoka, T.; Nawafune, H. Band Gap Engineering of CdTe

- Nanocrystals through Chemical Surface Modification *J. Am. Chem. Soc.* **2005**, *127*, 1634-1635.
- (26) Hughes, B. K.; Ruddy, D. A.; Blackburn, J. L.; Smith, D. K.; Bergren, M. R.; Nozik, A. J.; Johnson, J. C.; Beard, M. C. Control of PbSe Quantum Dot Surface Chemistry and Photophysics Using an Alkylselenide Ligand. *ACS Nano* **2012**, *6*, 5498-5506.
- (27) Fang, C.; van Huis, M. A.; Vanmaekelbergh, D.; Zandbergen, H. W. Energetics of Polar and Nonpolar Facets of PbSe Nanocrystals from Theory and Experiment *ACS Nano* **2010**, *4*, 211-218.
- (28) Gellen, T. A.; Lem, J.; Turner, D. B. Probing Homogeneous Line Broadening in CdSe Nanocrystals Using Multidimensional Electronic Spectroscopy. *Nano Lett.* **2017**, *17*, 2809-2815.
- (29) Reboredo, F. A.; Zunger, A. Surface-Passivation-Induced Optical Changes in Ge Quantum Dots. *Phys. Rev. B* **2001**, *63*, 235314-1–235314-7.
- (30) Poddubny, A. N.; Dohnalová, K. Direct band gap silicon quantum dots achieved via electronegative capping *Phys. Rev. B* **2014**, *90*, 245439-1– 245439-7.
- (31) Miura, N. *Physics of Semiconductors in High Magnetic Fields* Oxford science publications, OUP Oxford, 2008, ISBN: 0198517564, 9780198517566
- (32) Luo, J.-W.; Franceschetti, A.; Zunger, A. Quantum-Size-Induced Electronic Transitions in Quantum Dots: Indirect Band-Gap GaAs. *Phys. Rev. B* **2008**, *78*, 035306.
- (33) Wang, L.-W.; Zunger, A. Pseudopotential calculations of nanoscale CdSe quantum dots. *Phys. Rev. B* **1996**, *53*, 9579.
- (34) Fu, H.; Zunger, A. Local-density-derived semiempirical nonlocal pseudopotentials for InP with applications to large quantum dots. *Phys. Rev. B* **1997**, *55*, 1642.

- (35) Graf, P.A.; Kim, K.; Jones, W.B.; Wang, L.W. Surface Passivation Optimization Using DIRECT. *J. Comp. Phys.* **2007**, *224*, 824-835.
- (36) Anderson, N. C.; Hendricks, M. P.; Choi, J. J.; Owen, J. S. Ligand Exchange and the Stoichiometry of Metal Chalcogenide Nanocrystals: Spectroscopic Observation of Facile Metal-Carboxylate Displacement and Binding *J. Am. Chem. Soc.* **2013**, *135*, 18536-18548.
- (37) Califano, M. Characterisation of GaSb at the Nanoscale (unpublished).
- (38) García-Santamaría, F.; Chen, Y.; Vela, J.; Schaller, R. D.; Hollingsworth, J. a; Klimov, V. I. Suppressed Auger Recombination in "Giant" Nanocrystals Boosts Optical Gain Performance *Nano Lett.* **2009**, *9*, 3482-3488.
- (39)  $\Delta E$  accounts for ensemble structural effects - size distribution or shape anisotropy - and the influence of the nanocrystal environment - local electric fields and/or charge fluctuations.
- (40) Califano, M. Direct and Inverse Auger Processes in InAs Nanocrystals: Can the Decay Signature of a Trion Be Mistaken for Carrier Multiplication? *ACS Nano* **2009**, *3*, 2706-2714.
- (41) Schaller, R. D.; Pietryga, J. M.; Klimov, V. I. Carrier Multiplication in InAs Nanocrystal Quantum Dots with an Onset Defined by the Energy Conservation Limit *Nano Lett.* **2007**, *7*, 3469-3476.
- (42) Sills, A.; Harrison, P.; Califano, M. Exciton Dynamics in InSb Colloidal Quantum Dots. *J. Phys. Chem. Lett.* **2015** *7*, 31-35
- (43) Chang, A. Y.; Liu, W.; Talapin, D. V.; Schaller, R. D. Carrier Dynamics in Highly Quantum-Confined, Colloidal Indium Antimonide Nanocrystals *ACS Nano* **2014**, *8*, 8513-8519.

- (44) Calculated assuming a Gaussian broadening of 80 meV for the optical spectra.
- (45) Meinardi, F.; Colombo, A.; Velizhanin, K. A.; Simonutti, R.; Lorenzon, M.; Beverina, L.; Viswanatha, R.; Klimov, V. I.; Brovelli, S. Large-area luminescent solar concentrators based on 'Stokes-shift-engineered' nanocrystals in a mass-polymerized PMMA matrix. *Nat. Phot.* **2014**, *8*, 392-399.
- (46) Meinardi, F.; Ehrenberg, S.; Dharmo, L.; carulli, F.; Mauri, M.; Bruni, F.; Simonutti, R.; Kortshagen, U.; Brovelli, S. Highly efficient luminescent solar concentrators based on earth-abundant indirect-bandgap silicon quantum dots. *Nat. Phot.* **2017**, *11*, 177-185.
- (47) Buonsanti, R.; Milliron, D. J. Chemistry of Doped Colloidal Nanocrystals *Chem. Mater.* **2013**, *25*, 1305-1317.
- (48) Klimov, V. I. Optical Nonlinearities and Ultrafast Carrier Dynamics in Semiconductor Nanocrystals. *J. Phys. Chem. B* **2000**, *104*, 6112
- (49) Tu, C.-C.; Awasthi, K.; Chen, K.-P.; Lin, C.-H.; Hamada, M.; Ohta, N.; Li, Y.K. Time-Gated Imaging on Live Cancer Cells Using Silicon Quantum Dot Nanoparticles with Long-Lived Fluorescence. *ACS Photonics*, **2017**, *4*, 1306-1315.
- (50) We assume the radiative lifetime of the biexciton to be 4 times that of the single exciton and the only (or the most efficient) nonradiative pathway to be AR.<sup>51</sup>
- (51) Park, Y.-S.; Malko, A. V.; Vela, J.; Chen, Y.; Ghosh, Y.; Garcia-Santamaria, F.; Hollingsworth, J. A.; Klimov, V. I.; Htoon, H., Near-unity quantum yields of biexciton emission from CdSe/CdS nanocrystals measured using single-particle spectroscopy. *Phys. Rev. Lett.* **2011**, *106*, 187401/1-187401/4.
- (52) Beberwyck, B. J.; Alivisatos, A. P. Ion Exchange Synthesis of III-V Nanocrystals *J. Am. Chem. Soc.* **2012**, *134*, 19977-19980.

- (53) Lauth, J.; Strupeit, T.; Kornowski, A.; Weller, H. A Transmetalation Route for Colloidal GaAs Nanocrystals and Additional III-V Semiconductor Materials *Chem. Mater.* **2013**, *25*, 1377-1383.
- (54) Srivastava, V.; Liu, W. Y.; Janke, E. M.; Kamysbayev, V.; Filatov, A. S.; Sun, C. J.; Lee, B.; Rajh, T.; Schaller, R. D.; Talapin, D. V. Understanding and curing structural defects in colloidal GaAs nanocrystals. *Nano Lett.* **2017**, *17*, 2094-2101.
- (55) Lee, B. G.; Luo, J.-W.; Neale, N. R.; Beard, M. C.; Hiller, D.; Zacharias, M.; Stradins, P.; Zunger, A. Quasi-Direct Optical Transitions in Silicon Nanocrystals with Intensity Exceeding the Bulk. *Nano Lett.* **2016**, *16*, 1583-1589.

This material is available free of charge via the Internet at <http://pubs.acs.org>.